

Recyclable and Reprocessable Epoxy Vitrimer Adhesives

David Santiago,* Dailyn Guzmán, Jesús Padilla, Pere Verdugo, Silvia De la Flor, and Àngels Serra

Cite This: *ACS Appl. Polym. Mater.* 2023, 5, 2006–2015

Read Online

ACCESS |



Metrics & More



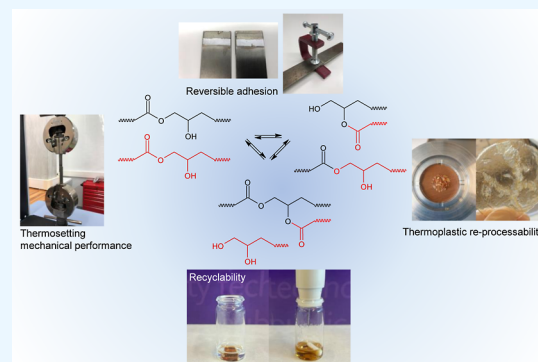
Article Recommendations



Supporting Information

ABSTRACT: Epoxy-based vitrimers represent a promising option toward sustainability and circular economy in automotive structural applications. In this work, a series of vitrimer materials are presented to be used as recyclable and reprocessable adhesives for such applications. These formulations consist of diglycidyl ether of bisphenol A-anhydride systems with glutaric anhydride and glycerol as cocuring agents in several proportions and 1,5,7-triazabicyclo[4.4.0]dec-5-ene (TBD) or 1-methylimidazole (1MI) as catalysts. The materials obtained revealed relatively high T_g s, up to 85 °C, as well as a homogeneous network structure. They also showed complete stress relaxation in times as short as just 3.6 min at 180 °C. The presence of TBD in the vitrimer allows the fastest relaxation. The thermosets were recycled and reprocessed through alcoholysis and mechanical grinding. These formulations were also applied as adhesives for mono- and multimaterial joints showing values of single-lap shear stress as high as those shown by commercial adhesives. Reversible adhesion was also studied after joint failure and after debonding without failure. In summary, the materials and methodology presented here represent a comprehensive study of recyclable and reprocessable epoxy-based vitrimers.

KEYWORDS: epoxy, thermosets, vitrimers, lightweight, recycling, adhesion



INTRODUCTION

The increasing demand for more efficient vehicles leads manufacturers to use lightweight materials such as high-strength steel, magnesium, and aluminum alloys or composites. Adhesively bonded joints are increasingly being used in the automotive industry mainly because they allow the joining of different materials and provide excellent thermal and insulation properties, good damping capacities, appreciable weight, noise reduction, and better corrosion resistance, in comparison with classic mechanical joints.^{1–4}

Adhesives used in structural applications include epoxy resins, anaerobic adhesives, acrylics, polyurethanes, silicones, and high-temperature adhesives such as phenolics, polyimides, and bismaleimides. Among them, epoxy-based adhesives possess high specific strength and excellent chemical and environmental resistance. Many efforts have been done to obtain recyclable, reprocessable, and healable epoxy materials. However, the presence of covalent bonds, which defines their three-dimensional network, prevents them to be reshaped, reprocessed, or recycled and thus makes their reparation difficult or even impossible. A new family of materials, called vitrimers, has been developed by Leibler and co-workers⁵ and has caught the attention of researchers because they combine the excellent performance of thermosets with some of the processability advantages of thermoplastics.^{5–7}

Vitrimers consist of three-dimensional polymeric structures with dynamic covalent bonds, which can lead to topological changes without affecting the average crosslinking degree. This

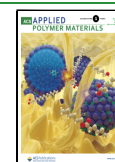
fact allows for reshaping, self-welding, reprocessing, and eliminating internal stresses, which appear during curing or service. In recent years, different reversible exchange reactions have been explored for the preparation of vitrimers, such as transesterification, transamination, disulfide exchange, transalkylation, siloxane equilibrium, dioxaborolane metathesis, amine–urea exchange, and transcarbamoylation.^{8–14}

The application of vitrimers as adhesives has grown in interest in recent years, mainly because of the possibility of obtaining self-healing and reweldable adhesives.^{15–18} The Arrhenius-type temperature dependence of the melt viscosity of vitrimers permits welding (or readhesion) while preserving the shape of the objects to be assembled. Numerous examples of welding of vitrimers of similar chemical nature have been described in the literature.^{15,17–22} Typically, welding of vitrimers that contain a higher concentration of exchangeable links yields greater weld strength. Increasing the temperature and/or the catalyst loading accelerates welding. The functional groups at the interface of two welded vitrimers are exchanged and not consumed while welding. Thus, if a joint debonds, it is possible to reform the joint without modifying the surface of

Received: November 30, 2022

Accepted: January 24, 2023

Published: February 6, 2023



the vitrimer by applying the appropriate stimulus while the two surfaces are in contact to repair the weld or rebond the joint.²³

This work proposes epoxy-anhydride vitrimeric systems as recyclable, reprocessable, and reweldable structural adhesives. Following the idea of Liu and co-workers,²⁴ a polyol monomer was introduced into the system, but unlike their work, we also used 5 mol % of the catalyst to ensure faster stress relaxation processes and a proper curing reaction.

One can find excellent works in the literature regarding the preparation and characterization of vitrimeric formulations with notable thermomechanical properties, structural adhesives, and multimaterial joints and also the recyclability of thermosetting materials and reversible adhesive joints. Table S1 (Supporting Information) enlists some of the most interesting studies about vitrimers and reversible adhesion. In the present work, we have prepared epoxy vitrimers with glass transition temperatures up to 85 °C, very short relaxation times, and very high lap-shear strength comparable to conventional commercial adhesives. Thanks to these characteristics, these materials were used as reversible adhesives for structural applications. Because of their excellent vitrimeric behavior, these materials can be recycled through dissolution and remolding. In addition, this work also includes single-lap shear adhesion tests with mono- and multimaterial adherents and two different methodologies for the study of reversible adhesion, readhesion after lap failure, and readhesion after debonding and the study of recycling and reprocessing of these materials. In summary, one can find in this work a complete study that gathers the preparation and characterization of transesterification-induced epoxy-based vitrimers and their application as reversible and recyclable adhesives.

EXPERIMENTAL METHODS

Materials. Diglycidyl ether of bisphenol A (DGEBA) (Araldite GY 240), with an epoxy equivalent of 182 g/mol, was purchased from Huntsman (Salt Lake City, UT, USA). Glutaric anhydride (GA), glycerol (Gly), 1,5,7-triazabicyclo[4.4.0]dec-5-ene (TBD), and ethylene glycol were purchased from Sigma-Aldrich (St. Louis, MO, USA). 1-Methylimidazole (IMI) was purchased from BASF (Ludwigshafen am Rhein, Germany). The chemical structures of the compounds used in the preparation of the formulations are depicted in Scheme S1 (Supporting Information).

Preparation of Formulations. Six formulations were prepared with different epoxy/anhydride molar ratios, polyol content, and two different catalysts. The composition of each formulation is detailed in Table S2 (Supporting Information). Two epoxy/anhydride molar ratios were chosen: a stoichiometric ratio between epoxy and anhydride groups (1:1) and another with an excess of epoxy groups (1:0.8). 15 and 20 mol % of glycerol to the anhydride content were used (0.15 and 0.2 Gly, respectively). The amount of catalyst (TBD or IMI) was chosen to be 5 mol % of the epoxy group content. The reason for using these ratios is simply fulfilling a compromise between relatively high glass transition temperatures (T_g s) as well as fast relaxation times (τ). Preliminary results demonstrated that decreasing the epoxy/anhydride ratio beyond 1:0.8 increased the T_g and τ to an unacceptable value. On the contrary, when a higher mol % of polyol was added, τ decreased until excellent values but so did the T_g .

First, the polyol and the anhydride were mixed at 140 °C for 1.5 h, the catalyst was added, and the formulation was mixed for an additional 10 min until a homogeneous mixture was obtained. The mixture was cooled to room temperature and mixed with the DGEBA monomer. Final formulations were degassed under vacuum conditions to avoid the appearance of bubbles during the curing reaction. Samples of final materials were obtained after curing for 3 h at 120 °C, 3 h at 160 °C, and 3 h at 180 °C using a Teflon mold. Samples were polished with sandpaper until reaching the desired dimensions.

Thermal Characterization. The study of the curing process was performed by differential scanning calorimetry (DSC) using a Mettler-Toledo DSC3+ 700/970 (Columbus, OH, USA) calorimeter calibrated using an indium standard (heat flow calibration) and an indium–lead–zinc standard (temperature calibration). A flow of N₂ at 100 mL/min was used, and the weight of the samples for the analysis was ~10 mg. The curing process was studied in non-isothermal mode at 10 °C/min from 30 to 270 °C. The glass transition temperatures (T_g s) of the samples once cured were determined in dynamic scans at 50 °C/min from –20 to 180 °C.

The thermal stability of cured samples was studied by thermogravimetric analysis (TGA), using a Mettler-Toledo TGA 2 thermobalance (Columbus, OH, USA). All experiments were performed under an inert atmosphere (N₂ at 100 mL/min). Pieces of the cured samples with an approximate mass of 10 mg were degraded between 30 and 600 °C at a heating rate of 20 °C/min.

Thermomechanical and Mechanical Characterization. Thermomechanical properties were measured using a TA Instruments DMA Q800 (New Castle, DE, USA) equipped with a tension film clamp. Prismatic rectangular samples of about 30 mm × 6 mm × 1.5 mm were analyzed at 1 Hz, 0.1% strain, and a heating rate of 3 °C/min from 0 to 150 °C. The storage modulus in the glassy state (E'_g) and rubbery state (E'_r) was obtained at 0 °C and $T_g + 50$ °C, respectively. The glass transition temperature (T_g) was determined from the maximum of the peak of $\tan \delta$, which is the ratio of loss modulus to elastic modulus and a measure of the energy dissipation.²⁵

Stress Relaxation Tests. Stress relaxation tests were carried out using a TA Instruments DMA Q800 (New Castle, DE, USA) equipped with a film tension clamp on samples with the same dimensions as previously defined. Samples were first equilibrated at 160 °C for 5 min, then a constant strain of 1.5% (this deformation is within the linear range) was applied to the sample, and the consequent stress level was monitored as a function of time. The process was repeated every 10 until 190 or 200 °C (depending on the catalyst used). The stress σ was normalized by the initial stress σ_0 , and the relaxation time τ was determined as the time necessary to relax 1/ e of the initial value σ_0 . The activation energy E_a was calculated for each material by using an Arrhenius-type equation

$$\ln(\tau) = \frac{E_a}{RT} - \ln(A)$$

where τ is the time needed to attain a given stress relaxation value of 1/ $e \cdot \sigma_0$, A is a pre-exponential factor, T is the absolute temperature, and R is the gas constant.

The topology freezing temperature of T_v can be obtained as the temperature at which the material reaches a viscosity of 10¹² Pa·s.²⁶ Nevertheless, for our system, T_v can be extrapolated fitting the Arrhenius equation to a relaxation time deduced from Maxwell's relation ($\eta = E' \cdot \tau$) assuming that E' (obtained from the DMA experiments) remains invariant in the rubbery state.

Creep Experiments. Creep and recovery properties were studied using a TA Instruments DMA Q800 (New Castle, DE, USA) equipped with a film tension clamp with the same dimensions as previously defined. A stress of 0.1 MPa was applied for 30 min at 120 °C, then the stress was immediately released, and the sample was left to recover for another 30 min. This procedure was repeated every 10 until 190 or 200 °C. The viscosity (η) was calculated using the following equation

$$\eta = \frac{\sigma}{\dot{\epsilon}}$$

The deformation rate was determined as the slope of the linear fit of the linear part of the variation of the strain as a function of time. The fragility Angell plot was then obtained by plotting η as a function of T_v/T .

Recycling and Reprocessing. For chemical recycling, samples of each material were cut into little pieces and then dissolved in ethylene glycol at 180 °C at a concentration of 30 wt % for 1 h and with an amount of catalyst corresponding to the 5 wt % of the polymer. The

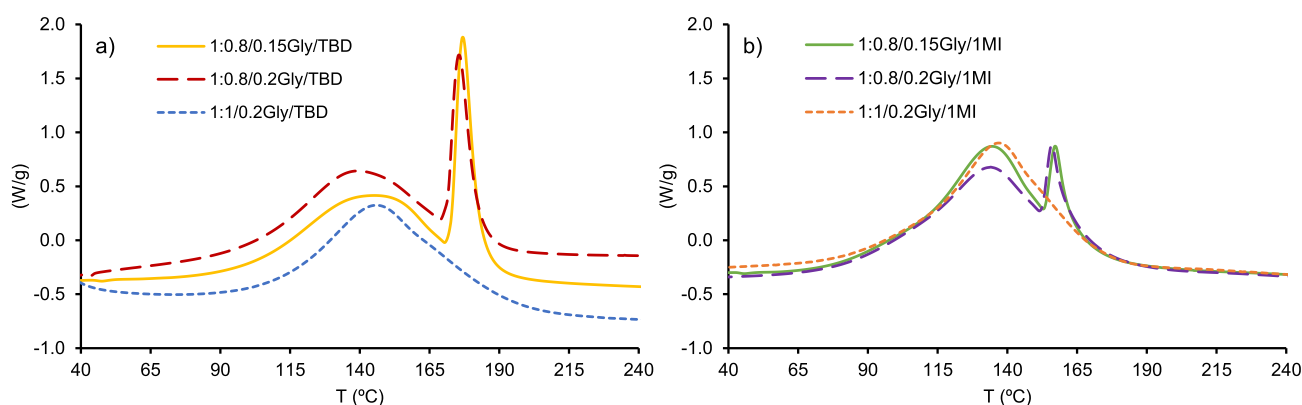


Figure 1. DSC thermograms corresponding to the dynamic curing at 10 °C/min of the materials studied of formulations with TBD (a) and with 1MI (b).

resultant dissolution was used to prepare new materials by evaporating ethylene glycol under vacuum conditions and pouring the viscous liquid obtained into a Teflon mold. A new material was obtained after curing at 180 °C for 6 h and 190 °C for 4 h. For mechanical recycling of vitrimers, materials were ground and put inside a metal mold covered with Teflon. Then, the powder was remolded after applying a pressure of 8.4 MPa at 180 °C for 3 h with a manual hydraulic press Specac Atlas 15T (Orpington, UK).

Adhesion Tests. Samples of stainless-steel DP1000 (ArcelorMittal, Luxembourg, Luxembourg) aluminum alloy 5754 (Aludium, Amstelveen, Holland) and carbon-epoxy prepreg Castro Composites MTC275 (Pontevedra, Spain) of 100 × 25 × 1.5 mm were used as adherents (Table S3, Supporting Information), according to the EN 1465:2009 standard. The surfaces of the substrates were prepared following the EN 13887:2004 standard. Overlapping regions of 12.5 mm were degreased with acetone to remove any greasy impurities. Then, mechanical abrasion with P180 sandpaper was performed by roughening the bond area. Surfaces were degreased with acetone again to remove any abrasion residue. Teflon spacers were used to ensure a bond line thickness of 0.2 mm as recommended by the standard. In addition, a constant pressure of 3 kPa was applied on the joints during curing to ensure good contact between adherents and adhesive. The final strength of the single-lap joints was evaluated by tensile lap-shear tests according to the standard EN 1465:2009. The geometry of the lap-shear joint specimens used is shown in Figure S1a (Supporting Information). The tests were performed using a universal testing machine Lloyd EZ50 (Bognor Regis, UK) equipped with a 50 kN load cell at a 1.3 mm/min crosshead speed. Five samples of each formulation were tested, and the average lap-shear strength was calculated. Two commercial adhesives for automotive applications, Teroson EP 5090 and Loctite EA 9514, were kindly given by Henkel (Düsseldorf, Germany) and tested for comparative purposes.

The procedures for studying readhesion are as follows. In the case of readhesion after lap failure, both parts of the single-lap joint sample were put together after being stretched until a break in a lap-shear test. A constant pressure of 8 MPa was applied to both halves by controlling the torque with a specifically designed assembly (Figure S1b, Supporting Information). In the case of readhesion after debonding, single-lap joint samples were placed at 180 °C for 1 h, and then, as the vitrimer was relaxed, they were pulled apart by hand. Again, both halves were put together with the assembly of Figure S1b and placed at 180 °C for 3 h for re-adhesion.

RESULTS AND DISCUSSION

Study of the Curing Process. Six different formulations, with the compositions detailed in Table S2, were prepared by mixing DGEBA, glycerol, and GA in the presence of a basic catalyst (TBD or 1MI). Anhydrides can react with epoxy and hydroxy groups, leading to a networked structure with ester and β -hydroxy ester groups. A stoichiometric ratio between

epoxy and anhydride groups (1:1) was selected and another with an excess of epoxy groups (1:0.8) so that a homopolymerization of epoxy groups took place and led to an increase of the glass-transition temperature (T_g).

In preparing the reactive formulation, the first step was the esterification of glycerol by anhydride to form a triester-triacid. The heating at 140 °C for 1.5 h ensures complete esterification of the hydroxyl groups.²⁴ This was confirmed by FTIR spectroscopy. In Figure S2a (Supporting Information), one can see the disappearance of the broad peak corresponding to OH groups of glycerol, centered at 3300 cm^{-1} , and the appearance of a very broad peak corresponding to OH groups of carboxylic acid around 3000 cm^{-1} .²⁷ In Figure S2b, the reduction of the peaks associated with anhydride groups around 1800 and 1760 cm^{-1} and the appearance of two peaks associated with carbonyl ester around 1740 cm^{-1} and C=O of carboxylic acid around 1700 cm^{-1} can be observed. It should be noted that, in all formulations, there is an excess of anhydride groups about the OH groups that in a further step can react with epoxides.

Several reactions occur in the curing process. Carboxylic acids react with epoxy groups to yield β -hydroxy ester linkages, anhydrides react with epoxy groups to form esters,²⁸ and in epoxy-rich formulations, homopolymerization leads to the formation of polyether structures.²⁹ In addition to these reactions, transesterification processes have been reported to lead to an increase in crosslinking density.³⁰

Figure 1 shows the DSC thermograms of formulations with TBD and 1MI (Figure 1a,b, respectively), and Table 1 collects the main calorimetric data obtained during the curing reactions. In formulations with an epoxy/anhydride ratio of 1:0.8, a homopolymerization reaction of the excess of epoxy groups can be observed at around 177 °C in formulations with TBD and around 156 °C in formulations with 1MI. From Figure 1 and Table 1, it can be observed that formulations with 1MI are slightly more reactive than formulations with TBD since both reaction processes (epoxy-carboxylic acid reaction and homopolymerization of epoxy groups) start at lower temperatures. The homopolymerization peak is much higher when TBD is used, indicating a faster process. Moreover, the peak area is more significant, indicating that more epoxide homopolymerization occurs. These facts are due to the highest nucleophilicity of TBD, acting as a catalyst and as an initiator. The curing enthalpies, which include both reactions, show values around 110 kJ per epoxy equivalent, which is in accordance with the enthalpy of epoxy-anhydride reactions described in the literature.²⁸

Table 1. Calorimetric Data of the Curing Process and Temperature of 2% of Weight Loss in an N₂ atmosphere of All the Formulations Studied

sample	T_{peak}^a (°C)	T_{peak}^b (°C)	ΔH^c (J/g)	ΔH^d (kJ/ee)	T_g^e (°C)	$T_{2\%}^f$ (°C)
1:1/0.2Gly/TBD	146		289	109	66	319
1:0.8/0.2Gly/TBD	140	176	374	110	76	314
1:0.8/0.15Gly/TBD	145	177	383	112	85	305
1:1/0.2Gly/1MI	137		369	111	68	309
1:0.8/0.2Gly/1MI	134	156	378	110	69	321
1:0.8/0.15Gly/1MI	135	157	383	110	75	345

^aTemperature of the maximum of the exotherm of the epoxy-anhydride reaction. ^bTemperature of the maximum of the exotherm of the epoxy homopolymerization reaction. ^cEnthalpy released during curing by gram. ^dEnthalpy released by an epoxy equivalent. ^eGlass transition temperature of the final cured material. ^fTemperature of 2% of weight loss in N₂.

As expected, the thermosetting materials obtained showed higher T_g s with lower glycerol content and a 1:0.8 epoxy-anhydride ratio (Table 1), with values up to 85 °C for formulation 1:0.8/0.15Gly/TBD. The differences are more notable in the samples catalyzed by TBD due to the higher contribution of the homopolymerization reaction that increases the crosslinking density and consequently the T_g .

In the past years, there have been published several different vitrimer systems. Among epoxy-anhydride or epoxy-carboxylic acid, some are elastomeric materials with T_g s around room temperature.^{15,19,31,32} More recently, high T_g vitrimeric epoxy systems have been reported but often show slow or insufficient transesterification reactions.^{33,34} Thus, a compromise between relatively high T_g and fast transesterification reaction rate should be reached for vitrimer networks to be applied in structural applications. In this sense, the networks presented in this work fulfill both requisites, as will be demonstrated.

Thermogravimetric Characterization. The materials prepared were characterized by thermogravimetry to study their stability at high temperatures. Figure 2a, b shows the weight loss curves and the derivatives of weight loss curves as a function of temperature in the N₂ atmosphere of formulations 1:1/0.2Gly/TBD and 1:1/0.2Gly/1MI. For the sake of simplicity, only these two formulations were plotted since all formulations showed similar trends with the same catalysts. The degradation curves are almost unimodal, with a single peak at high temperatures, indicating that all the degradation processes occur simultaneously. Table 1 collects the values of temperatures of initial weight loss ($T_{2\%}$), and it can be

observed that materials with 1MI showed slightly higher degradation temperatures than those prepared with TBD. From Figure 2b, it can be observed that the degradation rates are slower in formulations with TBD.

Thermomechanical Characterization. Thermomechanical characteristics were determined using DMA. Figure 3 shows the storage modulus (E') and $\tan \delta$ as a function of temperature for formulations with TBD (Figure 3a) and with 1MI (Figure 3b), and the main thermomechanical data obtained from these experiments are collected in Table 2. Formulations with TBD showed increasing T_g (determined as the peak of $T_{\tan\delta}$) either with an epoxy/anhydride ratio of 1:0.8 or with less glycerol. The bigger contribution of the homopolymerization of the excess of epoxy groups leads to an increased crosslinking density and, thus, to higher T_g . Conversely, a bigger amount of glycerol decreases the crosslinking density, leading to a decrease in T_g . In the case of formulations with 1MI, no significant changes are observed among them, and all materials showed T_g s around 66 °C. Despite the values of T_g , the tendency in the relaxed moduli indicates a decrease in the crosslinking density.

All formulations, either with TBD or 1MI, showed a high peak of $\tan \delta$ and very narrow transitions, with the FWHM around 10 °C in all cases (Table 2). Formulations with an epoxy/anhydride ratio of 1:1 showed a higher $\tan \delta$ peak and a slightly narrow transition because there was no homopolymerization reaction and only one curing process took place. These results are indicative of a homogeneous and mobile structure which is advantageous for materials to show vitrimeric behavior.³⁰

Vitrimeric Characterization. Leibler's group initially reported the vitrimeric characteristics of polyester networks,⁵ and then Williams and colleagues deeply studied them.^{30,31,35} The reaction of carboxylic groups with epoxides leads to the formation of β -hydroxy ester units, which facilitates the rearrangement of the network structure. The reaction behind this vitrimeric characteristic is the transesterification reaction (see Scheme S2, Supporting Information), which proceeds by the attack of the hydroxyl groups on the carbonyl ester, catalyzed by a tertiary amine.

Viscoelastic properties at high temperatures were studied using DMA with stress relaxation and creep tests. It is well known that the viscosity of vitrimers at high temperatures is controlled by a chemical exchange reaction, which leads to a temperature–viscosity relation that follows Arrhenius' law. This is the main difference between vitrimers and dissociative

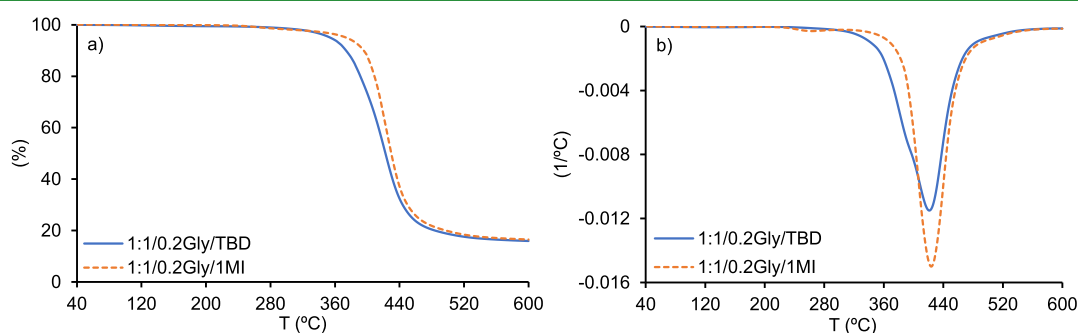


Figure 2. TGA (a) and differential thermogravimetry (b) of the formulations 1:1/0.2Gly/TBD and 1:1/0.2Gly/1MI under a N₂ atmosphere and 10 °C/min.

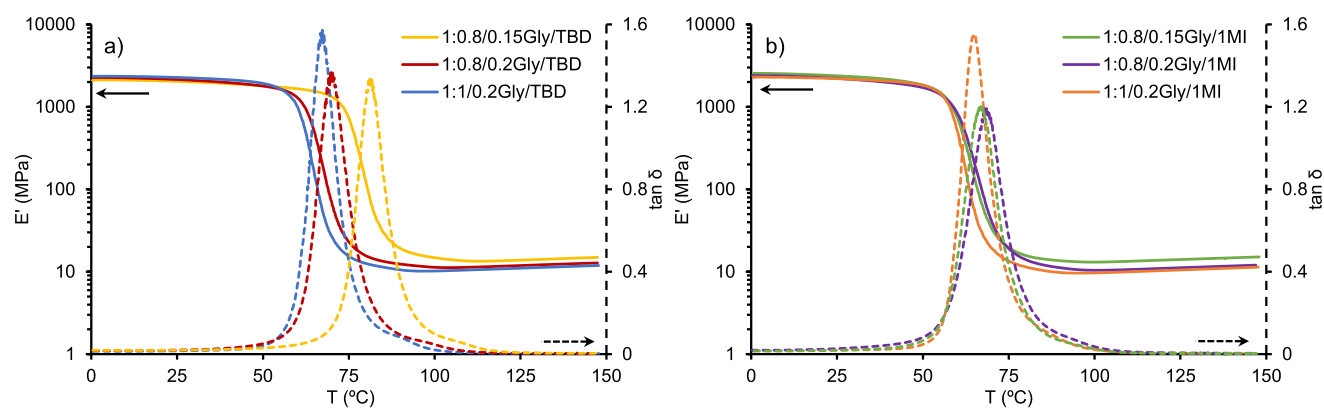


Figure 3. E' modulus and $\tan \delta$ as a function of the temperature of formulation with TBD (a) and with 1MI (b).

Table 2. Thermomechanical Data of the Thermosetting Polymers Prepared

sample	$T_{\tan \delta}^a$ (°C)	FWHM ^b (°C)	E_g^c (MPa)	E_r^d (MPa)
1:1/0.2Gly/TBD	64	9	2284	12
1:0.8/0.2Gly/TBD	70	11	2275	12
1:0.8/0.15Gly/TBD	81	10	2126	14
1:1/0.2Gly/1MI	65	10	2303	10
1:0.8/0.2Gly/1MI	68	12	2407	11
1:0.8/0.15Gly/1MI	67	12	2558	14

^aTemperature of the peak on $\tan \delta$. ^bFull width at half-maximum. ^cStorage modulus measured at $T_g - 50$ °C. ^dStorage modulus measured at $T_g + 50$ °C.

covalent adaptable networks since the latter show a sharp drop in viscosity at high temperatures.⁶

The vitrimeric behavior of a thermosetting material is asserted by determining the relaxation time (τ) at different temperatures for a stress relaxation of $\sigma/\sigma_0 = 1/e$. Figure 4a shows the stress relaxation curves at 180 °C for all the formulations studied, whereas Figure 4b shows stress relaxation curves between 160 and 200 °C for the formulation 1:0.8/0.2Gly/TBD at several temperatures. From the results shown in Figure 4a, it can be observed that the relaxation process is much faster with TBD rather than with 1MI. While formulation 1:1/0.2Gly/TBD took 4.4 min to relax to $\sigma/\sigma_0 = 1/e$, a similar formulation but with 1MI (1:1/0.2Gly/1MI) took 33.4 min. The relaxation times τ at 180 °C for all the

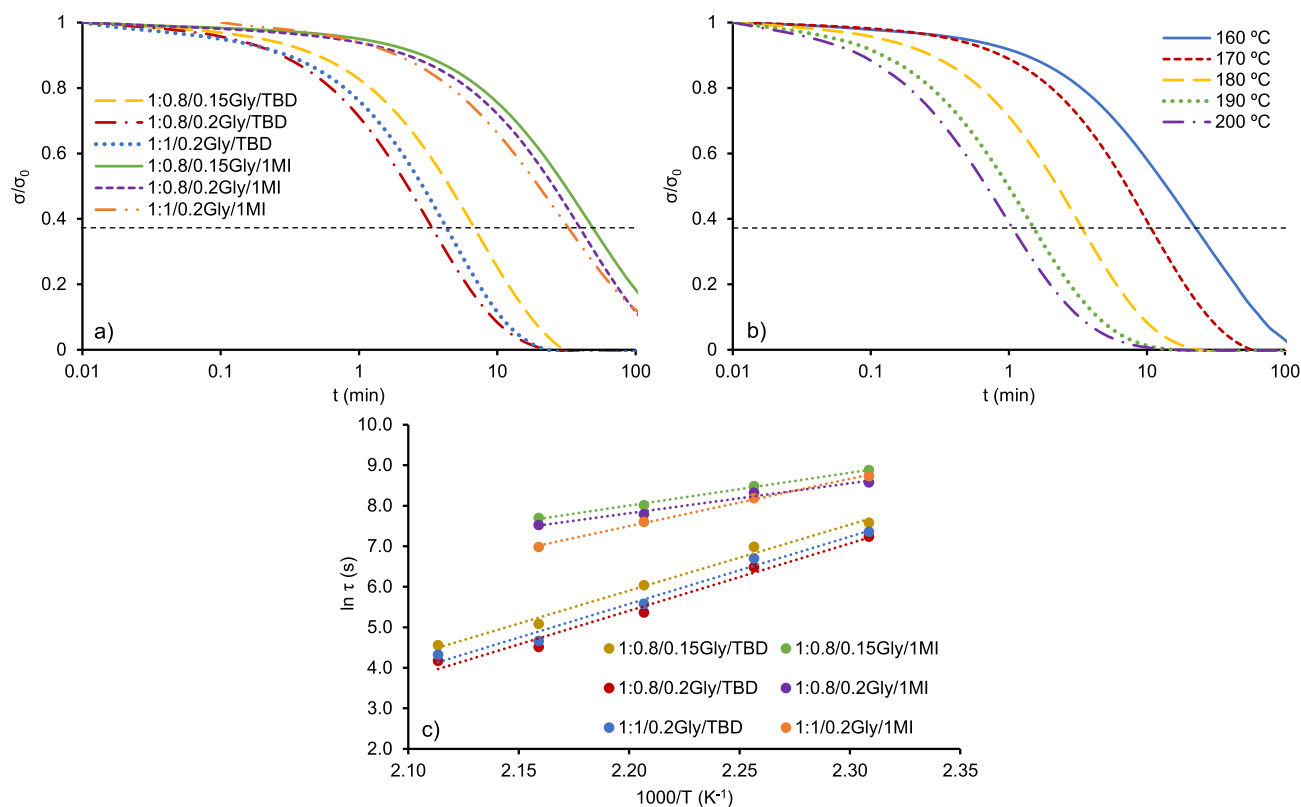


Figure 4. (a) Normalized stress relaxation as a function of time at 180 °C for each formulation studied; (b) normalized stress relaxation as a function of time at various temperatures for formulation 1:0.8/0.2Gly/TBD; (c) fitting of stress relaxation results to Arrhenius' equation for each formulation studied.

materials prepared are collected in Table 3. As can be observed, the type of catalyst has a significant effect on

Table 3. Time for Stress Relaxation at 180 °C, Topology Freezing Temperature (T_v), Activation Energy, and Arrhenius Adjusting Parameters of Each Formulation

sample	$\tau_{180^\circ\text{C}}$ (min)	T_v (°C)	E_a (kJ/mol)	$\ln A$ (s)	R^2
1:0.8/0.15Gly/TBD	7.0	120	135	29.93	0.99
1:0.8/0.2Gly/TBD	3.6	116	132	29.52	0.98
1:1/0.2Gly/TBD	4.4	118	138	31.02	0.98
1:0.8/0.15Gly/1MI	50.5	106	67	9.74	0.99
1:0.8/0.2Gly/1MI	40.3	97	62	8.48	0.98
1:1/0.2Gly/1MI	33.4	120	97	18.20	0.99

relaxation times. Formulations with 1MI showed τ values similar to those reported for similar systems.^{19,22,24,36} However, formulations with TBD showed remarkably lower values at 180 °C up to 3.6 min, which is significantly lower than those obtained by transesterification-induced epoxy-type vitrimeric systems. These results agree with the higher basicity and nucleophilicity of TBD ($pK_a = 14.4$, $N = 16.16$) in comparison to 1MI ($pK_a = 7.1$, $N = 11.9$)³⁷ that enhances the catalytic activity of TBD. From the relaxation times measured, we can see that the epoxy-rich materials relax more slowly since the proportion of β -hydroxy esters is lower and the crosslinking density higher due to the existence of the polyether structure formed by epoxy homopolymerization. It is important to highlight that the materials can experiment with complete relaxation in some minutes when an adequate temperature is selected.

By the Arrhenius equation, the activation energy of the exchange mechanism (E_a) and the topology freezing transition temperature (T_v) can be determined. Figure 4c shows the fitting of stress relaxation results to Arrhenius' equation for each formulation. These values are listed in Table 3, along with adjusting parameters.

There is a great difference in the activation energies between materials containing TBD and 1MI. While the activation energies of the TBD materials are high, those of 1MI are low, which contrasts with the shorter relaxation times of the TBD materials. However, this can be explained by the higher values of the pre-exponential factor in these materials. The lower activation energy values of the materials with 1MI lead, in general, to lower T_v values. All calculated T_v values are higher than the T_g values, indicating that the material must already

have a certain mobility before the chemical exchange process begins.

To further analyze viscoelastic properties at high temperatures, creep experiments were conducted. Figure 5a shows the creep behavior of the formulation 1:0.8/0.2Gly/TBD at 130 °C (around T_v) and 180 °C (well above T_v). Thermosets exhibit good resistance to creep, thanks to their permanent network structure, showing constant deformation when a constant external stress is applied, and almost no plastic deformation appears when the stress is released. This behavior was observed when tested around T_v (130 °C). However, when tested at $T > T_v$ (180 °C), the deformation increased progressively and presented plastic deformation when the stress was released due to topological rearrangements of the network structure. This behavior confirms that these vitrimers behave like viscoelastic liquids. From these tests, viscosity at different temperatures was determined and represented in the Angell fragility plot (Figure 5b). From Figure 5b, it can be observed that all formulations behave as strong liquids at temperatures above T_v .³⁸ This allows their reprocessing and recycling easily.

Recycling and Reprocessing. We used two approaches to recycle vitrimers in the present study, chemical and mechanical. The first approach involves the dissolution of the vitrimer in a mixture of a solvent and a catalyst. Samples like those prepared for the thermomechanical characterization were dissolved. They were neither cut nor ground. The solvent chosen was ethylene glycol because, at high temperatures (180 °C) and in the presence of a catalyst, a transesterification reaction can take place between OH groups of ethylene glycol and ester groups of vitrimers. In this case, ethylene glycol is not only the solvent but also the alcohol that attacks the ester group. Thus, the vitrimer sample is dissolved through alcoholysis. After 1 h approximately, the material was fully dissolved, and then the solvent in excess was removed at 180 °C under vacuum conditions. The viscous liquid obtained was then poured into a Teflon mold and cured again. Table 4 collects the thermal and thermomechanical data.

Compared with virgin vitrimers, the materials after CR showed a decrease in T_g between 17 and 34 °C in formulations with TBD and between 23 and 31 °C in formulations with 1MI (measured as the maximum of the $\tan \delta$ peak). A decrease in thermal stability can also be observed as a decrease in $T_{2\%}$ between 10 and 30 °C depending on the formulation. In all cases, the transition is wider and there is a decrease of an order of magnitude in the rubbery modulus E'_{cr} , which indicates, along with T_g values, a decrease in the crosslinking density.

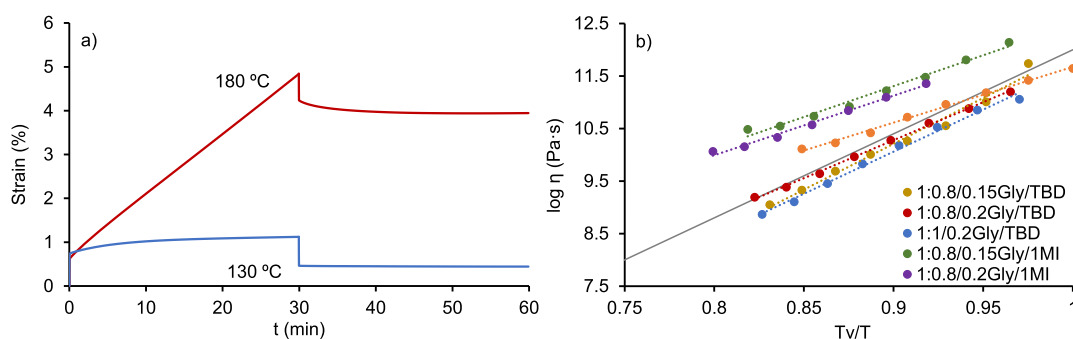


Figure 5. (a) Creep recovery curves at 130 and 180 °C for the formulation 1:0.8/0.2Gly/TBD. (b) Angell fragility plot of the logarithm of the viscosity as a function of T_v/T . For comparative purposes, an ideal strong liquid is included as a reference (gray line).³⁹

Table 4. Thermal and Thermomechanical Data of Formulations after Chemical Recycling (CR) and Mechanical Recycling (MR)

sample	T_g (°C)	$T_{2\%}$ (°C)	$T_{\tan\delta}$ (°C)	FWHM (°C)	E'_g (MPa)	E'_r (MPa)
CR_1:0.8/0.15Gly/TBD	59	267	47	20	890	0.9
CR_1:0.8/0.2Gly/TBD	55	286	52	22	653	0.7
CR_1:1/0.2Gly/TBD	54	272	47	19	2250	2.0
CR_1:0.8/0.15Gly/1MI	46	301	38	20	794	0.9
CR_1:0.8/0.2Gly/1MI	50	315	45	15	2530	1.6
CR_1:1/0.2Gly/1MI	44	314	34	15	2670	1.5
MR_1:0.8/0.15Gly/TBD	73	319	63	14	2300	8
MR_1:0.8/0.2Gly/TBD	62	303	58	15	1983	7
MR_1:1/0.2Gly/TBD	61	295	54	14	1426	4
MR_1:0.8/0.15Gly/1MI	62	304	62	15	2436	9
MR_1:0.8/0.2Gly/1MI	61	292	55	12	3166	11
MR_1:1/0.2Gly/1MI	60	279	59	14	3075	9

Table 5. Average Lap-Shear Strength of the First Adhesion and Rewelded Samples of Each Formulation Studied with DP1000 Steel Adherents and Average Lap-Shear Strength of Formulations 1:0.8/0.2Gly/1MI with Multimaterial Adherents

sample	first adhesion (kN)	readhesion after failure (kN)	readhesion after debonding (kN)	adherents	1:0.8/0.2Gly/1MI (kN)
Teroson EP 5090	10.7 ± 0.2			steel–steel	8.6 ± 0.3
Loctite EA 9514	9.8 ± 0.3			aluminum–aluminum	3.6 ± 0.3
1:0.8/0.15Gly/TBD	9.1 ± 0.2	3.0 ± 0.4	8.1 ± 0.6	CFRP–CFRP	1.3 ± 0.2
1:0.8/0.2Gly/TBD	9.3 ± 0.1	4.1 ± 0.5	6.2 ± 0.2	aluminum–steel	6.1 ± 0.2
1:1/0.2Gly/TBD	8.1 ± 0.3	2.2 ± 0.5	5.2 ± 0.6	aluminum–CFRP	3.6 ± 0.2
1:0.8/0.15Gly/1MI	8.6 ± 0.2	3.0 ^a	2.7 ± 0.3	steel–CFRP	2.5 ± 0.1
1:0.8/0.2Gly/1MI	8.6 ± 0.3	2.5 ± 0.1	3.3 ± 0.1		
1:1/0.2Gly/1MI	8.1 ± 0.3	2.8 ± 0.3	4.3 ± 0.2		

^aOnly one representative result was obtained.

There is no clear tendency in E'_g values since they depend on the solubility process and solvent evaporation. This result is due to the excess of ethylene glycol and the possibility to react by both OH groups or only by one. Thus, the crosslinking density is reduced, and consequently, T_g and moduli also decrease. However, the chemical structure should be comparable.

However, this CR process is very attractive to recycling fiber-reinforced composites or to recovering the fibers, which is a crucial step forward to the circular economy and sustainable lightweight materials.^{40–42}

The mechanical approach for recycling vitrimers consists in grinding the samples into small pieces and remolding them by applying pressure and temperature. Table 4 enlists the most important thermal and thermomechanical data. The changes suffered by recycled materials are lower with mechanical recycling than with CR. There is, obviously, a decrease in T_g s and $T_{2\%}$ s but not as high as in the case of CR because of the fact explained above. The curve of the glass transition is slightly wider than in virgin materials, and E'_g and E'_r values show a slight decrease or none. It should be considered that the harsh conditions of the pressing process and the grinding of the samples destroy not only reversible bonds but also permanent ones, which certainly affect the thermal and thermomechanical properties of recycled thermosets. Since this recycling process involves grinding the materials, it is not possible to recycle composite matrices. Notwithstanding, it can be adopted in other applications without fibers, such as in adhesives.

Adhesion. Table 5 collects the average results of lap-shear adhesion strength of the formulations studied as well as the results of both commercial adhesives. All vitrimers studied showed an average lap-shear strength between 8 and 9 kN,

which is almost as high as in the case of commercial adhesives (~10 kN), but these have no vitrimeric behavior. Formulations with an excess of epoxy groups (ratio epoxy/anhydride of 1:0.8) showed slightly higher lap-shear strength. No significant differences were found between formulations with different catalysts. Figure S3 (Supporting Information) shows the failure surface of 1:1/0.2Gly/TBD and 1:1/0.2Gly/1MI joints that failed cohesively close to the interface.^{43,44} The rest of the adhesive joints showed the same failure mode.

Thanks to the self-healable behavior of vitrimers, after the adhesion tests, the two halves of the single lap joint sample can be rejoined again by putting together both parts and applying the same conditions of mechanical recycling (180 °C and 8.4 MPa for 3 h). However, the viscoelastic properties at high temperatures of vitrimers also allow dismantling of the joint and rebonding again. The results of the readhesion after failure and after debonding are shown in Table 5. There is no standard method to quantify the ability of readhesion of a vitrimer adhesive. Many studies opt for custom tests,^{15,17,18,24,30} but from the point of view of the authors, the best method is to reproduce the test according to the EN 1465:2009 standard but with the remended single lap joint samples. The values of lap-shear after readhesion are not particularly high. In the case of readhesion after failure, the reason might be the plastic deformation of the adherents and the necessity to ensure a perfect fit between the adhesive layers of both adherents, which is often difficult. In the case of readhesion after debonding, the values of lap shear are significantly higher in formulations with TBD reaching values up 89% concerning the first lap-shear value (Table 5).

Table 5 also shows the results of the multimaterial adherents lap-shear tests with the adhesive 1:0.8/0.2Gly/1MI. The failure

load increases with the adherent yield strength (Table S3, Supporting Information).

A significant drawback associated with single-lap joints is the presence of stress concentrations at the end of the overlap, which causes the joint to rotate and expose the adhesive to shear and peeling stresses, and it may lead to premature joint failure.⁴⁵ As the plastic deformation of the adherent decreases, the adhesive can develop its full shear strength capacity and show higher joint strength.⁴⁴ Thus, the best results were obtained with steel–steel and aluminum–steel adherents. Figure S4a (Supporting Information) shows the results of the aluminum adherent after failure. As can be observed, the plastic deformation of the adherent is notorious, which means that the effect of peel stress is more significant.⁴⁶ This explains the decrease in aluminum–steel and aluminum–aluminum joints with respect to steel–steel joints.

In the case of joints with CFRP adherents, although there was no significant plastic deformation after failure, the failure surface of the joint revealed the presence of voids caused by an inappropriate wetting process. This was also observed with steel–CFRP and aluminum–CFRP joints. The results with CFRP adherents reveal the necessity of appropriate surface treatment for this kind of adherent since mechanical abrasion was not adequate (Figure S4b, Supporting Information).

CONCLUSIONS

In this work, a series of epoxy-based vitrimer materials were prepared with a commercial DGEBA as an epoxy monomer, glycerol and GA as curing agents, and 1-methylimidazole and 1,5,7-triazabicyclo[4.4.0]dec-5-ene as catalysts. These materials showed excellent results in terms of thermal and thermomechanical properties, recycling and reprocessing conditions, as well as adhesion.

Calorimetric studies showed high T_g s, up to 85 °C, and the thermomechanical characterization revealed very homogeneous networks. These materials can undergo topological rearrangements through transesterification reactions and show complete and very fast stress relaxation at temperatures around 180 °C. This behavior allowed these materials to be recycled and reprocessed. CR was accomplished by the alcoholysis of the vitrimers in ethylene glycol and mechanical recycling by grinding the samples of vitrimers and remolding them. These materials were also tested as adhesives in mono- and multimaterial joints. The results obtained revealed high adhesion strength, as high as in the case of commercial adhesives, but also put the dependency of lap-shear adhesion tests on adherent's yield stress and surface treatments in evidence.

Finally, these materials have shown a good compromise between thermal, thermomechanical, and vitrimeric properties to be applied in structural applications and lightweight technologies, such as matrix composites or adhesives, but with the possibility of separate inorganic fibers from polymeric matrices of composites, dismantle and reweld adhesion joints, or remold samples of these materials.

ASSOCIATED CONTENT

Supporting Information

The Supporting Information is available free of charge at <https://pubs.acs.org/doi/10.1021/acsapm.2c02063>.

Comparison between the material's performance of the present work and other vitrimer networks of the

literature; schemes of the chemical structure of the compounds used to prepare the formulations; percentages in weight of the components used in the preparation of formulations; mechanical properties of the adherent materials; scheme of the single-lap joint test specimen with dimensions and assembly used for readhesion tests; FTIR spectra of glycerol and the mixture of GA and 20% of glycerol after 1.5 h at 140 °C; and FTIR spectra of GA and the mixture of GA and 20% of glycerol after 1.5 h at 140 °C; scheme of the transesterification reaction; failure surface of the joints prepared with formulations 1:1/0.2Gly/TBD and 1:1/0.2Gly/1MI; and plastic deformation of the aluminum adherent after failure and failure surface of the CFRP–CFRP joints (PDF)

AUTHOR INFORMATION

Corresponding Author

David Santiago – *Eurecat-Chemical Technologies Unit, Tarragona 43007, Spain; Department of Mechanical Engineering, Universitat Rovira i Virgili, Tarragona 43007, Spain; orcid.org/0000-0002-1687-5536; Email: david.santiago@eurecat.org*

Authors

Dailyn Guzmán – *Eurecat-Chemical Technologies Unit, Tarragona 43007, Spain*

Jesús Padilla – *Department of Analytical and Organic Chemistry, University Rovira i Virgili, Tarragona 43007, Spain*

Pere Verdugo – *Eurecat-Chemical Technologies Unit, Tarragona 43007, Spain; Department of Analytical and Organic Chemistry, University Rovira i Virgili, Tarragona 43007, Spain; orcid.org/0000-0003-1019-5406*

Silvia De la Flor – *Department of Mechanical Engineering, Universitat Rovira i Virgili, Tarragona 43007, Spain; orcid.org/0000-0002-6851-1371*

Àngels Serra – *Department of Analytical and Organic Chemistry, University Rovira i Virgili, Tarragona 43007, Spain; orcid.org/0000-0003-1387-0358*

Complete contact information is available at: <https://pubs.acs.org/doi/10.1021/acsapm.2c02063>

Author Contributions

D. S. and D. G. contributed equally to this paper. J. P. and P. V. prepared the formulations and carried out the characterization. S. D. and À. S. revised and edited the manuscript. The manuscript was written through the contributions of all authors. All authors have given approval to the final version of the manuscript.

Funding

This work is part of the R&D project PID2020-115102RB-C21 funded by MCNI/AEI/10.13039/501100011033; we acknowledge this grant and the Generalitat de Catalunya (2017-SGR-77).

Notes

The authors declare no competing financial interest.

REFERENCES

- (1) Banea, M. D.; da Silva, L. F. M. Adhesively Bonded Joints in Composite Materials: An Overview. *Proc. Inst. Mech. Eng., Part L* 2009, 223, 1–18.

- (2) de Queiroz dos Reis, M.; Banea, M. D.; da Silva, L. F. M.; Carbas, R. J. C. Mechanical Characterization of a Modern Epoxy Adhesive for Automotive Industry. *J. Braz. Soc. Mech. Sci. Eng.* **2019**, *41*, 340.
- (3) Avendaño, R.; Carbas, R. J. C.; Marques, E. A. S.; da Silva, L. F. M.; Fernandes, A. A. Effect of Temperature and Strain Rate on Single Lap Joints With Dissimilar Lightweight Adherends Bonded With an Acrylic Adhesive. *Compos. Struct.* **2016**, *152*, 34–44.
- (4) Banea, M. D.; Rosioara, M.; Carbas, R. J. C.; da Silva, L. F. M. Multi-Material Adhesive Joints for Automotive Industry. *Composites, Part B* **2018**, *151*, 71–77.
- (5) Montarnal, D.; Capelot, M.; Tournilhac, F.; Leibler, L. Silica-Like Malleable Materials From Permanent Organic Networks. *Science* **2011**, *334*, 965–968.
- (6) Denissen, W.; Winne, J. M.; Du Prez, F. E. Vitrimers: Permanent Organic Networks With Glass-Like Fluidity. *Chem. Sci.* **2016**, *7*, 30–38.
- (7) Kloxin, C. J.; Bowman, C. N. Covalent Adaptable Networks: Smart, Reconfigurable and Responsive Network. *Chem. Soc. Rev.* **2013**, *42*, 7161–7173.
- (8) Denissen, W.; Rivero, G.; Nicolaÿ, R.; Leibler, L.; Winne, J. M.; Du Prez, F. E. Vinylous Urethane Vitrimers. *Adv. Funct. Mater.* **2015**, *25*, 2451–2457.
- (9) Canadell, J.; Goossens, H.; Klumperman, B. Self-healing Materials Based on Disulfide Links. *Macromolecules* **2011**, *44*, 2536–2541.
- (10) Hendriks, B.; Waelkens, J.; Winne, J. M.; Du Prez, F. E. Poly(thioether) Vitrimers via Transalkylation of Trialkylsulfonium Salts. *ACS Macro Lett.* **2017**, *6*, 930–934.
- (11) Wu, X.; Yang, X.; Yu, R.; Zhao, X. J.; Zhang, Y.; Huang, W. A Facile Access to Stiff Epoxy Vitrimers With Excellent Mechanical Properties Via Siloxane Equilibration. *J. Mater. Chem. A* **2018**, *6*, 10184–10188.
- (12) Röttger, M.; Domenech, T.; van der Weegen, R.; Breuillac, A.; Nicolaÿ, R. L.; Leibler, L. High-Performance Vitrimers From Commodity Thermoplastics Through Dioxaborolane Metathesis. *Science* **2017**, *356*, 62–65.
- (13) Erice, A.; Ruiz de Luzuriaga, A.; Matxain, J. M.; Ruipérez, F.; Asua, J. M.; Grande, H.-J.; Rekondo, A. Reprocessable and Recyclable Crosslinked Poly(urea-urethane)s Based on Dynamic Amine/Urea Exchange. *Polymer* **2018**, *145*, 127–136.
- (14) Zheng, N.; Fang, Z.; Zou, W.; Zhao, Q.; Xie, T. Thermoset Shape-Memory Polyurethane with Intrinsic Plasticity Enabled by Transcarbamoylation. *Angew. Chem., Int. Ed.* **2016**, *128*, 11593–11597.
- (15) Zhao, S.; Abu-Omar, M. M. Catechol-Mediated Glycidylation toward Epoxy Vitrimers/Polymers with Tunable Properties. *Macromolecules* **2019**, *52*, 3646–3654.
- (16) Zhang, S.; Liu, T.; Hao, C.; Wang, L.; Han, J.; Liu, H.; Zhang, J. Preparation of a Lignin-Based Vitriimer Material and Its Potential Use for Recoverable Adhesives. *Green Chem.* **2018**, *20*, 2995–3000.
- (17) Trejo-Machin, A.; Puchot, L.; Verge, P. A Cardanol-Based Polybenzoxazine Vitriimer: Recycling, Reshaping and Reversible Adhesion. *Polym. Chem.* **2020**, *11*, 7026–7034.
- (18) Ji, F.; Liu, X.; Sheng, D.; Yang, Y. Epoxy-Vitriimer Composites Based on Exchangeable Aromatic Disulfide Bonds: Reprocessibility, Adhesive, Multi-Shape Memory Effect. *Polymer* **2020**, *197*, 122514.
- (19) Wu, J.; Yu, X.; Zhang, H.; Guo, J.; Hu, J.; Li, M.-H. Fully Biobased Vitrimers from Glycyrrhizic Acid and Soybean Oil for Self-Healing, Shape Memory, Weldable, and Recyclable Materials. *ACS Sustain. Chem. Eng.* **2020**, *8*, 6479–6487.
- (20) Zhou, Z.; Su, X.; Liu, J.; Liu, R. Synthesis of Vanillin-Based Polyimine Vitrimers with Excellent Reprocessability, Fast Chemical Degradability, and Adhesion. *ACS Appl. Polym. Mater.* **2020**, *2*, 5716–5725.
- (21) Tang, J.; Wan, L.; Zhou, Y.; Pan, H.; Huang, F. Strong and Efficient Self-Healing Adhesives Based on Dynamic Quaternization Cross-Links. *J. Mater. Chem. A* **2017**, *5*, 21169–21177.
- (22) Han, J.; Liu, T.; Hao, C.; Zhang, S.; Guo, B.; Zhang, J. A Catalyst-Free Epoxy Vitriimer System Based on Multifunctional Hyperbranched Polymer. *Macromolecules* **2018**, *51*, 6789–6799.
- (23) Van Zee, N. J.; Nicolaÿ, R. Vitrimers: Permanently Crosslinked Polymers with Dynamic Network Topology. *Prog. Polym. Sci.* **2020**, *104*, 101233.
- (24) Liu, T.; Zhang, S.; Hao, C.; Verdi, C.; Liu, W.; Liu, H.; Zhang, J. Glycerol Induced Catalyst-Free Curing of Epoxy and Vitriimer Preparation. *Macromol. Rapid Commun.* **2019**, *40*, 1800889.
- (25) Menard, K. P.; Menard, N. R. Dynamic Mechanical Analysis in the Analysis of Polymers and Rubbers, John Wiley & Sons, 2015.
- (26) Dyre, J. C. Colloquium: The Glass Transition and Elastic Models of Glass-Forming Liquids. *Rev. Mod. Phys.* **2006**, *78*, 953–972.
- (27) Pretsch, E.; Bühlmann, P.; Badertscher, M. *Structure Determination of Organic Compounds: Tables of Spectral Data*; 4th Ed.; Springer Berlin: Heidelberg, 2009.
- (28) Foix, D.; Yu, Y.; Serra, À.; Ramis, X.; Salla, J. M. Study on the Chemical Modification of Epoxy/Anhydride Thermosets Using a Hydroxyl Terminated Hyperbranched Polymer. *Eur. Polym. J.* **2009**, *45*, 1454–1466.
- (29) Fernández-Francos, X.; Cook, W. D.; Serra, À.; Ramis, X.; Liang, G. G.; Salla, J. M. Crosslinking of Mixtures of DGEBA with 1,6-Dioxaspiro[4,4]nonan-2,7-dione Initiated by Tertiary. Part IV. Effect of Hydroxyl Groups on Initiation and Curing Kinetics. *Polymer* **2010**, *51*, 26–34.
- (30) Altuna, F. I.; Hoppe, C. E.; Williams, R. J. J. Epoxy Vitrimers with a Covalently Bonded Tertiary Amine as Catalyst of the Transesterification Reaction. *Eur. Polym. J.* **2019**, *113*, 297–304.
- (31) Altuna, F. I.; Pettarin, V.; Williams, R. J. J. Self-Healable Polymer Networks Based on the Cross-Linking of Epoxidized Soybean Oil by an Aqueous Citric Acid Solution. *Green Chem.* **2013**, *15*, 3360–3366.
- (32) Capelot, M.; Montarnal, D.; Tournilhac, F.; Leibler, L. Metal-Catalyzed Transesterification for Healing and Assembling of Thermosets. *J. Am. Chem. Soc.* **2012**, *134*, 7664–7667.
- (33) Liu, T.; Hao, C.; Zhang, S.; Yang, X.; Wang, L.; Han, J.; Li, Y.; Xin, J.; Zhang, J. A Self-Healable High Glass Transition Temperature Bioepoxy Material Based on Vitriimer Chemistry. *Macromolecules* **2018**, *51*, 5577–5585.
- (34) Giebler, M.; Sperling, C.; Kaiser, S.; Duretek, I.; Schlögl, S. Epoxy-Anhydride Vitrimers from Aminoglycidyl Resins with High Glass Transition Temperature and Efficient Stress Relaxation. *Polymers* **2020**, *12*, 1148.
- (35) Altuna, F. I.; Hoppe, C. E.; Williams, R. J. J. Epoxy Vitrimers: The Effect of Transesterification Reactions on the Network Structure. *Polymers* **2018**, *10*, 43.
- (36) Yang, X.; Guo, L.; Xu, X.; Shang, S.; Liu, H. A Fully Bio-Based Epoxy Vitriimer: Self-Healing, Triple-Shape Memory and Reprocessing Triggered by Dynamic Covalent Bond Exchange. *Mater. Des.* **2020**, *186*, 108248.
- (37) Maji, B.; Stephenson, D. S.; Mayr, H. Guanidines: Highly Nucleophilic Organocatalysts. *ChemCatChem* **2012**, *4*, 993–999.
- (38) Urbain, G.; Bottinga, Y.; Richet, P. Viscosity of Liquid Silica, Silicates and Alumino-Silicates. *Geochim. Cosmochim. Acta* **1982**, *46*, 1061–1072.
- (39) Kelton, K. F. Kinetic and Structural Fragility—A Correlation Between Structures and Dynamics in Metallic Liquids and Glasses. *J. Phys.: Condens. Matter* **2017**, *29*, 023002.
- (40) Zhao, S.; Abu-Omar, M. M. Recyclable and Malleable Epoxy Thermoset Bearing Aromatic Imine Bonds. *Macromolecules* **2018**, *51*, 9816–9824.
- (41) Ruiz de Luzuriaga, A.; Martin, R.; Markaide, N.; Rekondo, A.; Cabañero, G.; Rodríguez, J.; Odriozola, I. Epoxy Resin with Exchangeable Disulfide Crosslinks to Obtain , Repairable and Recyclable Fiber-Reinforced Thermoset Composites. *Mater. Horiz.* **2016**, *3*, 241–247.

(42) Yu, K.; Shi, Q.; Dunn, M. L.; Wang, T.; Qi, H. J. Carbon Fiber Reinforced Thermoset Composite with Near 100% Recyclability. *Adv. Funct. Mater.* **2016**, *26*, 6098–6106.

(43) Anyfantis, K. N.; Tsouvalis, N. G. Loading and Fracture Response of CFRP-to-Steel Adhesively Bonded Joints with Thick Adherents - Part I: Experiments. *Compos. Struct.* **2013**, *96*, 850–857.

(44) da Silva, L. F. M.; Carbas, R. J. C.; Critchlow, G. W.; Figueiredo, M. A. V.; Brown, K. Effect of Material, Geometry, Surface Treatment and Environment on the Shear Strength of Single Lap Joints. *Int. J. Adhes. Adhes.* **2009**, *29*, 621–632.

(45) Durodola, J. F. Functionally Graded Adhesive Joints—A Review and prospectsProspects. *Int. J. Adhes. Adhes.* **2017**, *76*, 83–89.

(46) Kafkalidis, M. S.; Thouless, M. D. The Effects of Geometry and Material Properties on the Fracture of Single Lap-Shear Joints. *Int. J. Solid Struct.* **2002**, *39*, 4367–4383.

Recommended by ACS

High-Performance Epoxy Vitrimers with the Joint Action of Dual Dynamic Covalent Bonds

Xiaoyu Huang, Zixi Wang, *et al.*

DECEMBER 12, 2023

ACS APPLIED POLYMER MATERIALS

READ 

Robust Biobased Vitrimers and Its Application to Closed-Loop Recyclable Carbon Fiber-Reinforced Composites

Jiyae Hong, Munju Goh, *et al.*

SEPTEMBER 05, 2023

ACS SUSTAINABLE CHEMISTRY & ENGINEERING

READ 

Exploring the Limits of High- T_g Epoxy Vitrimers Produced through Resin-Transfer Molding

Vincent Schenk, Marc Guerre, *et al.*

SEPTEMBER 22, 2023

ACS APPLIED MATERIALS & INTERFACES

READ 

Recoverable Rosin-Based Epoxy Vitrimers with Robust Mechanical Properties and High Thermostability

Zhaoyi Luo, Yanning Zeng, *et al.*

SEPTEMBER 25, 2023

ACS APPLIED POLYMER MATERIALS

READ 

Get More Suggestions >